



Pyrolysis of biosolids with waste cardboard: effect of operating parameters, feedstock size and blending ratio

S. Zuhara¹ · S. Pradhan¹ · G. McKay¹

Received: 8 November 2022 / Revised: 30 March 2023 / Accepted: 22 April 2023 / Published online: 6 May 2023
 © The Author(s) 2023

Abstract

Global waste is a rising problem that requires attention. Pyrolysis is a process that converts waste into valuable products like biochar, bio-oil, and gas by heating feeds above 300 °C. Pyrolysis studies mostly concentrate on fuel production and characterization, while biochar studies lack parametric analysis, especially for co-pyrolysis. Little attention is given to the effects of blending ratio and particle size on biochar yield. This research focuses on the pyrolysis of biosolids obtained from gas-to-liquid wastewater treatment, waste cardboard, and co-pyrolysis of blended samples. Pyrolysis was performed using a muffled furnace at temperatures ranging from 350–850 °C, heating rates of 3–10 °C/min, and residence times of 30–180 min to examine biochar yield and properties. Particle sizes and blending ratios were also studied. Proximate and ultimate analyses, metal composition, surface area, and surface charge studies were conducted on biochar samples utilizing analytical instruments. Biosolids had the highest yield followed by mixed samples and cardboard for all conditions, with temperature and blending ratio having the greatest impact on yield. Regarding surface area, the maximum was found to be at 650 °C revealing 10.34, 170.4, and 124.8 m²/g for biosolids, cardboard, and mixed samples, respectively. A significant effect with change in blending ratio and a minimal effect by varying particle size was observed on the biochar yield. For future applications, temperatures below 550 °C can be considered in terms of biochar yield, ash, and metal contents; as heating rate and residence time showed minimal effects on yield, lower points are preferred to conserve energy during pyrolysis. Overall, mixing waste improved quality and yield, making it environmentally beneficial for applications.

Graphical abstract



Editorial responsibility: Fatih ŞEN.

Extended author information available on the last page of the article



Keywords Co-pyrolysis · Biomass · Surface area · Temperature · Heating rate

Abbreviations

BS	Biosolid
CB	Cardboard
HR	Heating rate
(ICP-OES)	Inductively coupled plasma optical emission spectroscopy
RT	Residence time
SA	Surface area
SS	Sewage sludge
TGA	Thermogravimetric analysis
DTG	Derivative thermogravimetric
GTL	Gas to liquids
ASTM	American Society for Testing and Materials
BET	Brunauer–Emmett–Teller
C	Carbon
H	Hydrogen
N	Nitrogen
O	Oxygen

Introduction

The global increase in population is proportional to the amount of waste being generated. The millions of tons of organic and inorganic wastes, both municipal and industrial wastes being dumped, are responsible for harmful environmental emissions (Nowicki et al. 2016). Global problems like climate change, land degradation, and environmental pollution lead to economic, social, and environmental instability. In recent times, the circular economy concept is gaining attraction to maximize the use of resources and hence reduce climate change impacts. Converting waste to value-added products supports this ideology by achieving a country's sustainability goals and increasing economic revenue (Mariyam et al. 2022). This seems more beneficial than other waste management techniques, such as landfilling and incineration that are considered environmentally harmful methods.

Thermochemical conversion of wastes is being increasingly investigated and applied around the world. Pyrolysis, which is one of the methods, focuses on converting wastes to products, including gas, oil, and char in the presence of an inert atmosphere from temperatures ranging from 300 to 900 °C (Ayyadurai and Arunachalam 2022; Mariyam et al. 2022; Saravanakumar et al. 2022). Pyrolysis of lignocellulosic materials and biomass to fuels (oil and gas)

and char started gaining recognition in the mid-1970s; the reasons being due to increasing energy demand, rise in petrol prices, and the need for clean energy due to climate change (Raju 2016). Research reveals that biochar often considered a by-product has prominent commercial applications for agricultural and water treatment purposes. In recent years, due to the increase in wastewater being produced, pyrolysis studies using wastewater treatment generated waste—biosolids or sewage sludge is gaining interest with a wide range of applications from carbon sequestration, soil fertilizers, and nutrients, to pollution treatment among others (Raju 2016).

Several operating parameters are crucial in determining the quantity and quality of the products obtained during pyrolysis. Often, the temperature is reported as the primary parameter that affects the products; lower temperature leads to higher char yields, whereas higher temperature yields more oil, gas, and ash products after pyrolysis (Brindhadevi et al. 2021). Furthermore, the heating rate, usually classified as slow and fast pyrolysis processes, yields higher char and fuel products (Yogalakshmi et al. 2022). Residence time is also considered one of the parameters affecting the formation and distribution of products generated at different temperatures (Yogalakshmi et al. 2022). Recently, co-pyrolysis, which is the pyrolysis of two or more wastes combined, is gaining attention as it helps reduce the waste volume effectively, and in some cases, also improves the quality of char produced (Zhang et al. 2020).

Despite the several applications of biochar, research on co-pyrolysis heavily resides in biofuel, more specifically, bio-oil production and optimization (Sakulkit et al. 2020; Mohamed and Li 2022). Additionally, a significant portion of studies focus on kinetics, thermal behavior of degradation, and synergistic studies (Thibanyane et al. 2019; Liu et al. 2020; Mariyam et al. 2022). Biochar related co-pyrolysis studies focus on yield studies based on several operational parameters (Rathnayake et al. 2021; Wantaneeeyakul et al. 2021). However, there is a lack of studies focusing on the effect of blending ratios and particle size of feeds on biochar yield. Furthermore, the implications of adding wastes with contrasting properties for co-pyrolysis needs to be investigated further, as the physical and chemical properties of the biochar influence their suitability for utilization in a significant way (Fakayode et al. 2020). When it comes to the feeds, lignocellulosic wastes



are considered to a great extent due to the presence of cellulose, hemicellulose, and lignin, which converts to solid, liquid, and gases by thermal decomposition in an efficient manner (Yogalakshmi et al. 2022). Even though there has been a variety of lignocellulosic feeds studied for co-pyrolysis, they are primarily region-centric wastes such as rice husk (Kazemi Targhi et al. 2022), bamboo waste (Li et al. 2020), and corn straw (Suo et al. 2021) among others. Therefore, this study focuses on cardboard, which is a common waste available all around the world. As mentioned before, due to the interesting output from biosolids (Callegari and Capodaglio 2018; Racek et al. 2020; Gopinath et al. 2021), the other waste considered for this co-pyrolysis study is biosolids. More specifically, this study utilizes biosolids from the largest gas-to-liquids (GTL) plant in Qatar, producing 6000 tons per year annually (Kogbara et al. 2020). Since the feeds seem to have different origins, understanding the structure, degradability, and optimization is essential before further applications.

This study is carried out in Qatar in the year 2022, and the following are the objectives of this study:

1. To characterize the feeds: biosolids (BS) and cardboard (CB) to understand the surface morphology, elemental composition, calorific value, pH, and surface area.
2. To understand the thermal degradation behavior of BS and CB and how the biochar properties change when the two feedstocks are mixed.
3. To study the effect of operating parameters (temperature, heating rate: HR, residence time: RT) and the feedstock particle size and blending ratio on the biochar yield for all three samples.
4. To understand the effect temperature has on the samples' ash content, surface charge, and metal content.
5. Finally, to observe the effect of the aforementioned operating parameters, feedstock particle size, and blending ratio on the biochar samples' surface area and elemental composition.

Materials and methods

Feedstock procurement

The BS samples were obtained from one of the gas-to-liquids (GTL) plants in Qatar operated by Shell Qatar, and the CB waste (1-ply) was collected from a leading shopping market in Qatar.

Feedstock characterization

Proximate analysis

Proximate analysis was conducted on samples using a thermal analyzer (SDT650, TA Instruments) according to the American Society for Testing and Materials, (ASTM D7582-15, ASTM International 2015) method. The samples, weighing an average 10 mg, were prepared in triplicates and heated in an inert environment starting from 105 °C for 30 min to determine moisture content. The temperature was then increased at a rate of 30 °C/min to 950 °C and held at this temperature for 7 min before oxygen was introduced to allow combustion for 10 min, enabling the ash content to be determined. Equation 1 was used to calculate the fixed carbon content. Proximate analysis was also performed on biochar samples produced from pyrolysis and co-pyrolysis at various temperatures, residence times, and heating rates to assess the effects of these parameters on ash content.

$$\begin{aligned} \text{Fixed carbon (\%)} \\ = 100\% - \text{Volatile matter (\%)} + \text{Ash (\%)} + \end{aligned} \quad (1)$$

Elemental analysis

The carbon (C), nitrogen (N), and hydrogen (H) content of the samples before and after pyrolysis were determined using an elemental analyzer (combustion type) (EA 3000, EuroVector). The samples were measured at 980 °C with a carrier flow of 121 mL/min. Oven-dried samples (0.50 to 1.5 mg) were weighed using acetanilide as a reference standard. The oxygen content was calculated based on the weight difference in elements, and the ash content obtained from the samples' total mass. The aromaticity and polarity were assessed by calculating the ratios of H/C and O/C.

pH measurement

The pH of the sample was determined using a modified ASTM standard method D3838-99 (ASTM, 217 2005). Specifically, 0.1 g of the dried sample was added to a beaker containing 10 mL of boiling de-ionized water and sealed in a tube for approximately 15 min. The pH was calculated using a filtered sample (Whatman paper, No. 2, 110 mm diameter) at 323 ± 5 K.



Thermogravimetric analysis (TGA)

The sieved single and mixed feeds (1:1) samples (1000 μm) were used to conduct a TGA run using a thermogravimetric analyzer (SDT650, TA Instruments) at 5 $^{\circ}\text{C}/\text{min}$ HR from room temperature to 900 $^{\circ}\text{C}$. The runs were accomplished under an N_2 atmosphere purged at 100 ml/min. Each run was conducted three times to ensure the reproducibility and accuracy of the results. The analysis provides results in the form of TGA and derivative thermogravimetric (DTG) curves, which helps study the thermal degradation behavior of the samples.

Nitrogen adsorption–desorption studies

The surface area (SA) of a material was determined using the Brunauer-Emmett-Teller (BET) method, which involved measuring the amount of nitrogen sorption at a temperature of 77 K and a relative pressure ranging from 0.05 to 0.35; the Nova 2200e surface area analyzer (Tristar3200, Micromeritics, USA) was used for this purpose. Prior to the analysis, the samples were degassed at a temperature of 105 $^{\circ}\text{C}$ for 480 min. The pore volume was also estimated using the BET method, based on the liquid adsorbate volume of nitrogen at a relative pressure of 0.99.

Calorific value measurement

The calorific values of the samples were determined using a 6300 Fixed Bomb Parr calorimeter, which operated under an oxygen atmosphere to facilitate combustion. To measure the calorific values, approximately 0.6 g of dried samples were placed in the bomb along with a magnetic thread, and 4000 psi of oxygen was added. The bomb was then immersed in 2 L of water, and the resulting temperature increase was measured using a variety of instruments including mercury-in-glass thermometers, platinum resistance thermometers, quartz oscillators, and thermistor systems.

Metal analysis

To determine the concentration and stability of metals in the samples, the feedstock's metal content was analyzed in triplicate. Initially, 0.3 g of each sample was digested in a microwave digester tank with 9 mL of pure nitric acid and 1 mL of H_2O_2 for 30 min. After shaking the mixture well, it was left to settle for 1 h after tightening the piston before being placed in the High-Performance Microwave Digestion System (Milestone, I-24100, Italy). Following digestion, the samples were cooled and diluted tenfold before analysis

using inductively coupled plasma optical emission spectroscopy (ICP-OES) (The Agilent 5800 ICP-OES, USA).

Surface characterization

To understand the surface characteristics of the samples, scanning electron microscopy (SEM) and energy-dispersive X-ray spectroscopy (EDS) techniques were utilized. The samples were in powder form and were spread onto carbon tape with excess powder removed by compressed air. The samples were coated with a thin layer of gold (using Quorum Q150 sputter) to allow for electrical conductivity and then analyzed using an ETD secondary electron detector and Quanta 650FEG FEI SEM. Elemental microanalysis was conducted using a Bruker Quantax EDS detector, with gold being removed to obtain a semi-quantitative result at 15 kV.

Experimental procedures

Sample preparation for pyrolysis

The samples are directly ground, sieved, and mixed to the desired ratios for all studies. For co-pyrolysis studies for understanding the effects of particle size (at temp: 450 $^{\circ}\text{C}$, HR: 5 $^{\circ}\text{C}/\text{min}$, 120 min), both samples are equally mixed (1:1) along with the single wastes; the particle sizes are: 355–710 μm (labelled-BS₃₅₅/CB₃₅₅/Mix₃₅₅), 710–1000 μm (labelled-BS₇₁₀/CB₇₁₀/Mix₇₁₀), and 1000–2000 μm (labelled-BS₁₀₀₀/CB₁₀₀₀/Mix₁₀₀₀). To accurately measure the particle size of the samples, a steel test sieve (ASTME 11 Standard ISO 565, USA) is used after grinding the samples. Furthermore, the co-pyrolysis blending ratio experiments are carried out by mixing BS and CB different blending ratios: 25% of BS and 75% CB (Mix₂₅), 50% mix (Mix₅₀), and 75% BS and 25% CB (Mix₇₅), all using 355–710 μm particle size samples (at temp: 450 $^{\circ}\text{C}$, HR: 5 $^{\circ}\text{C}/\text{min}$, 120 min). Both the above-described studies were carried out at 450 $^{\circ}\text{C}$ at a HR of 5 $^{\circ}\text{C}/\text{min}$ and a RT of 120 min.

Operating conditions

This section includes the conditions chosen for pyrolysis and co-pyrolysis studies involving temperature, HR and RT studies. In order to see the effect of these parameters on co-pyrolyzed chars, a 1:1 ratio of BS and CB was considered. The particle size used for all the parametric studies was 355–710 μm . For understanding the effects of temperature, the range selected was between 350 and 850 $^{\circ}\text{C}$ with 5 $^{\circ}\text{C}/\text{min}$ intervals. Alternatively, the HR studies included 3, 5, 8, and 10 $^{\circ}\text{C}/\text{min}$ and RT studies focused on 30, 60, 120, and



Table 1 Operating conditions for pyrolysis and co-pyrolysis studies

Parameter	Operating condition (varying)	Fixed conditions	Sample name
Temperature	350, 450, 550, 650, 750, 850 °C	HR: 5 °C /min RT: 120 min Blending ratio: 50:50 Particle size: 355–710 µm	Biosolids (BS ₃₅₀ –BS ₈₅₀) Cardboard (CB ₃₅₀ –CB ₈₅₀) Mixed (50:50) (Mix ₃₅₀ –Mix ₈₅₀)
HR	3, 5, 8, 10 °C /min	Temperature: 450 °C RT: 120 min Blending ratio: 50:50 Particle size: 355–710 µm	Biosolids (BS ₃ –BS ₁₀) Cardboard (CB ₃ –CB ₁₀) Mixed (50:50) (Mix ₃ –Mix ₁₀)
RT	30, 60, 120, 180 min	HR: 5 °C /min Temperature: 450 °C Blending ratio: 50:50 Particle size: 355–710 µm	Biosolids (BS ₃₀ –BS ₁₈₀) Cardboard (CB ₃₀ –BS ₁₈₀) Mixed (50:50) (Mix ₃₀ –Mix ₁₈₀)

180 min (all conducted at 450 °C), ensuring a wide range for char production. For each condition specified in Table 1, approximately 50 g of untreated samples were placed in a ceramic dish and then inserted into a pyrolysis furnace. The furnace used was a UL standard 1200 °C compact split tube furnace model (OTF-1200X-S, MTI Corporation). For all the cases, the temperature was regularly checked on the monitor of the muffled furnace; the instrument was maintained regularly for accurate temperature control during the pyrolysis process.

Yield calculation

The prepared samples (triplicates) were pyrolyzed under different conditions described in Table 1 in the presence of nitrogen using a muffle furnace (Lindberg Blue M-3504, Thermo Scientific) in batch mode as described in “[Operating conditions](#)” section. After pyrolysis, the cooled samples were used to calculate the yield by the equation below. The yield is calculated as follows:

$$\text{Biochar Yield (\%)} = \frac{\text{Biochar weight(g)}}{\text{Feed weight(g)}} \times 100 \quad (2)$$

Statistical analysis of the data obtained from the parametric study was uploaded on Excel and then exported to SPSS version 20 for statistical analysis. The main objective was to find out if there is a significant effect of varying parameters on char yield by conducting a Pearson correlation analysis.

Comparison studies

The biochar samples were characterized to understand the elemental composition following methodology in [Elemental analysis](#) section, SA using the methodology

in “[Nitrogen adsorption–desorption studies](#)” section, the content of metals in the biochar samples (BS_{350–550}, CB_{350–550}, Mix_{350–550}) were determined following methodology in “[Metal analysis](#)” section, and the effect of temperature on ash content as per in “[Proximate analysis](#)” section. The charge of the biochar samples was determined using a zeta potential analyzer (Malvern Panalytical Zetasizer Nano-ZS). To prepare the samples, 0.1 g of the char sample was added to 200 mL of distilled water to create a suspension of 0.5 ppm. The suspension was mixed thoroughly by shaking at 150 rpm for 12 h, after which the samples were transferred into a cuvette and analyzed using the zeta potential analyzer.

Results and discussion

Feedstock characterization

Proximate and ultimate analysis

BS and CB samples were analyzed to understand the content of moisture, volatile matter, ash, and fixed carbon by proximate analysis (Table S1). The moisture and fixed carbon contents of BS are slightly higher than those reported in the literature (Wang et al. 2016; Bai et al. 2021), showing a higher moisture content than CB, both under 13%. As expected, the volatile matter in the CB is higher than BS; the fixed carbon, however, is in the same range for all samples, all compliant with the values reported in the literature (Salvador et al. 2004; Sotoudehnia et al. 2021). Furthermore, the ultimate analysis showed the carbon content is higher in CB compared to BS (Salvador et al. 2004; Sukarta et al. 2018). Additionally, CB is revealed to have significantly higher oxygen content due to the reduced ash



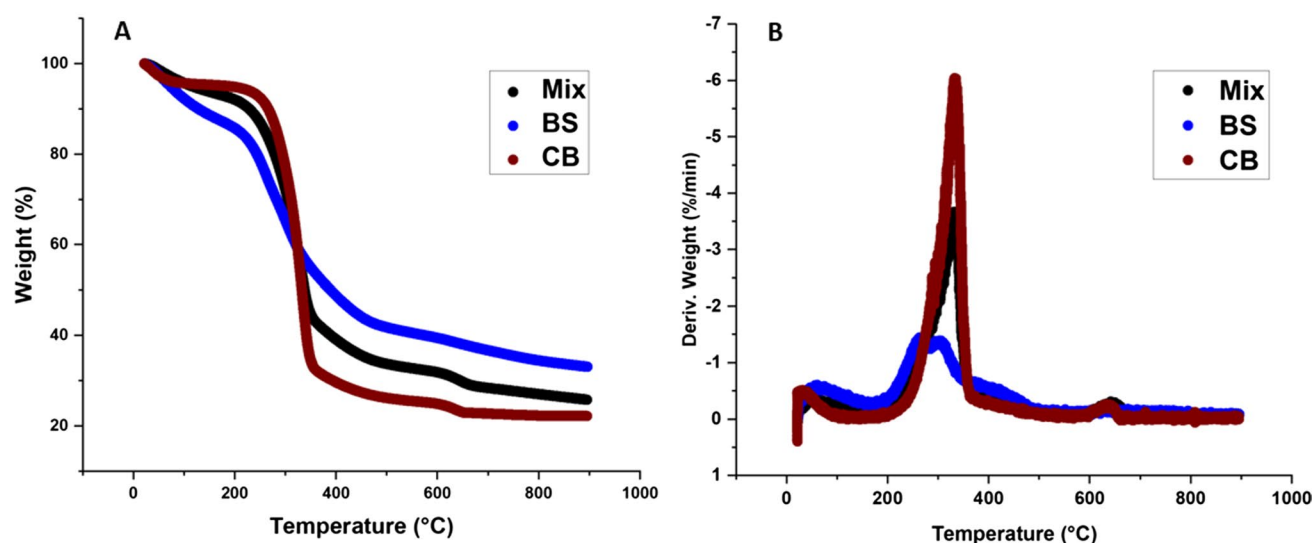


Fig. 1 Thermal degradation behavior of BS, CB, and mixed (50:50) feedstocks **A** TGA curve **B** DTG curve

content. The H/C and O/C calculated values show that the ratios decreased in the order BS > CB owing to the increasing carbon content. The nitrogen content, as predicted, is very low for CB as it has low protein content (Sotoudehnia et al. 2020); the nitrogen content in the BS sample is 5.03%, consistent with reported values (Wang et al. 2016; Patel et al. 2019). This information will be valuable in understanding the influence of surface functional groups if used for water treatment or bioremediation.

Thermal degradation behavior

The thermal degradation behavior of BS, CB and mixed (50:50) samples were studied by TGA. Figure 1A shows that the degradation behavior of all three samples is similar, showing significant weight loss between 400 and 500 °C. The degradation behavior divided into three stages reveals that the weight loss percent for the mixed sample is between the weight loss percentages of the single feedstocks at all stages. The weight loss % varies with the stages, as expected, BS samples have higher moisture

content which is apparent in the first dehydration/evaporation stage (Table 2); the second stage reveals that CB samples have the most volatile fraction with about 65% weight loss. The derivative thermogravimetric (DTG) curve in Fig. 1B shows a high peak in the second stage between 200 and 400 °C, indicating the presence of cellulose, hemicellulose, and lignin (primarily observed in biomass samples). The small hump in the final stage between 600 and 650 °C in the CB and mixed samples shows that some residual lignin is being degraded. Finally, the weight loss at the final stage, mainly describing the char degradation stage, reveals that weight loss for all three samples in the final stage was in the range of 7 and 8%. A similar trend is observed in the TGA studies for BS (Patel et al. 2019) and CB (Sotoudehnia et al. 2020) reported in the literature.

Feed characteristics

BS and CB were both found to be neutral, leaning toward alkaline in nature; BS had a pH of 8.13 ± 0.2 , which is

Table 2 Thermal degradation behavior of BS, CB, and mixed samples

Sample	Stage I	Weight loss (%)	Stage II	Weight loss (%)	Stage III	Weight loss (%)	Residual weight (%)	Total weight loss (%)
BS	Room temp—171.42	12.573	171.42—513.17	46.011	513.17—900	8.361	33.055	66.945
CB	Room temp—173.79	4.897	173.79—401.58	65.525	401.58—900	7.338	22.24	77.76
Mix	Room temp—172.11	6.922	172.11—494.45	59.236	494.45—900	8.063	25.779	74.221



slightly higher than the reported value of 8.03 pH (Chow and Pan 2020); alternatively, the recorded pH of CB was $\text{pH } 7.41 \pm 0.2$, which in accordance with the literature value of 7.69 (Suthar and Kishore Singh 2022). Furthermore, the calorific value for the BS sample is measured as 19.45 MJ/kg, which is around the range of 12 and 20 MJ/kg for BS (Collivignarelli et al. 2019). Similarly, the calorific value for CB was recorded as 17.06 MJ/kg, which is close to the value of 18 MJ/kg for corrugated cardboard (Sotoudehnia et al. 2020).

Regarding the metal content in the samples, both feedstocks had no detectable amounts of selenium, arsenic, and cadmium. Due to its nature, BS has a higher metal concentration than CB. Table S2 shows that CB has a limited amount of zinc and iron compared to BS; BS had an expectedly high concentration of iron as an iron coagulant was used during the industrial wastewater treatment process—a study revealed increased iron concentrations due to the usage of iron in the sewage pumping stations for controlling odors and corrosion (Morf et al. 2018).

The SA of the feedstock samples is 0.010, 1.74, and 0.560 m^2/g for BS, CB, and mixed samples, respectively. The SA of BS and CB is reported to be less than 3 m^2/g in the literature (Rio et al. 2006; Sotoudehnia et al. 2021). The surface morphology from the SEM images shows a distinct difference between the feeds—while BS is flat and non-porous given its origin, cardboard samples are revealed to be fibrous in nature (Fig. 2). From the SEM-EDS results, the BS in this

study detected nitrogen and sulfur mainly from the wastewater source. Additionally, iron was identified in the BS, similar to the metal analysis results. On the other hand, CB mainly detected carbon and oxygen, with the remaining elements below 0.72 (relative atom %) (Fig. 2).

Yield calculations

Figure S1 shows the BS, CB, and mixed samples before and after pyrolysis, and Fig. 3 shows the effect of temperature, HR, and RT on yields of BS, CB, and mixed samples. BS samples provide the highest yield at a maximum of 50% at 350 °C. It is clear in the case of BS that as temperature increases, the yield of biochar reduces significantly for all three samples. A study on mixed SS and municipal solid wastes at temperatures 350, 550, and 750 °C showed a drop in yield from 82, 62, and 60% (Wang et al. 2021). This study reveals a drastic yield drop after 550 °C, and the least yield ($\approx 5\%$) was obtained at 850 °C when CB was pyrolyzed (Fig. 3A). Increasing the pyrolysis temperature makes the chemical energy contained in the gases and liquids rather than in the char leading to lower char yields (Mašek et al. 2013).

The yield trend for varying heating rates (HR) was similar to that of temperature (Fig. 3B); however, it was more pronounced for the CB and mixed samples. Contrary to the effects of temperature and HR, the impact of

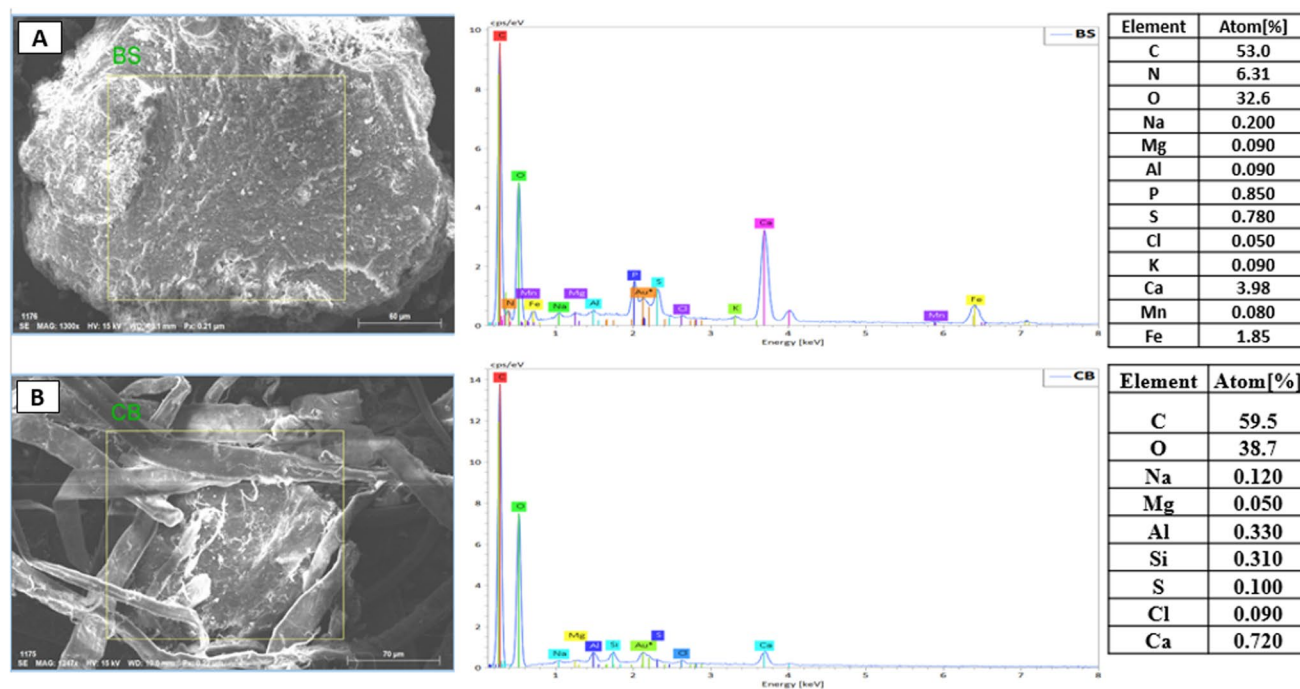


Fig. 2 SEM-EDS results of feeds **A** BS **B** CB



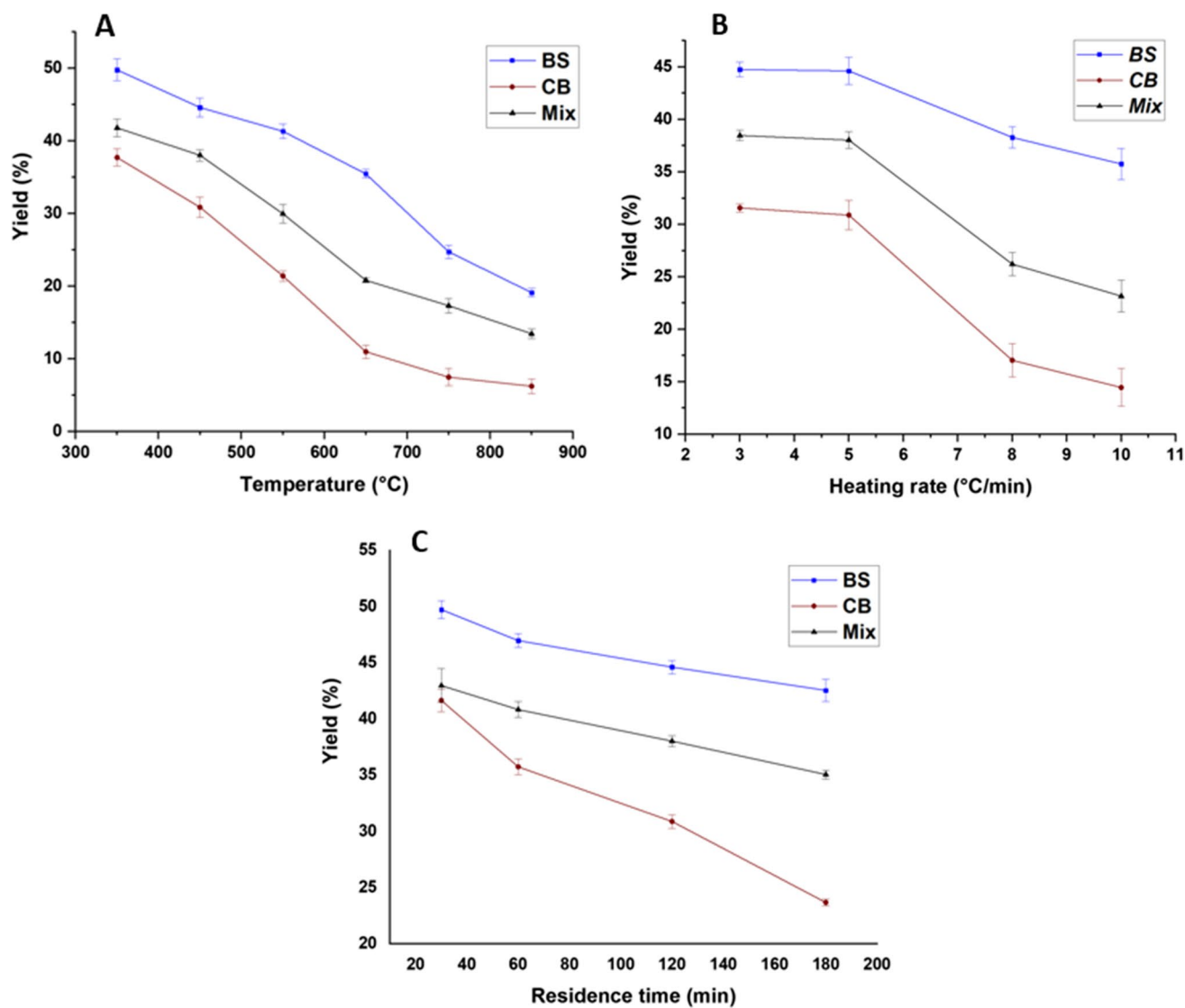


Fig. 3 Pyrolysis operating parameters effect on yield **A** temperature **B** HR **C** RT

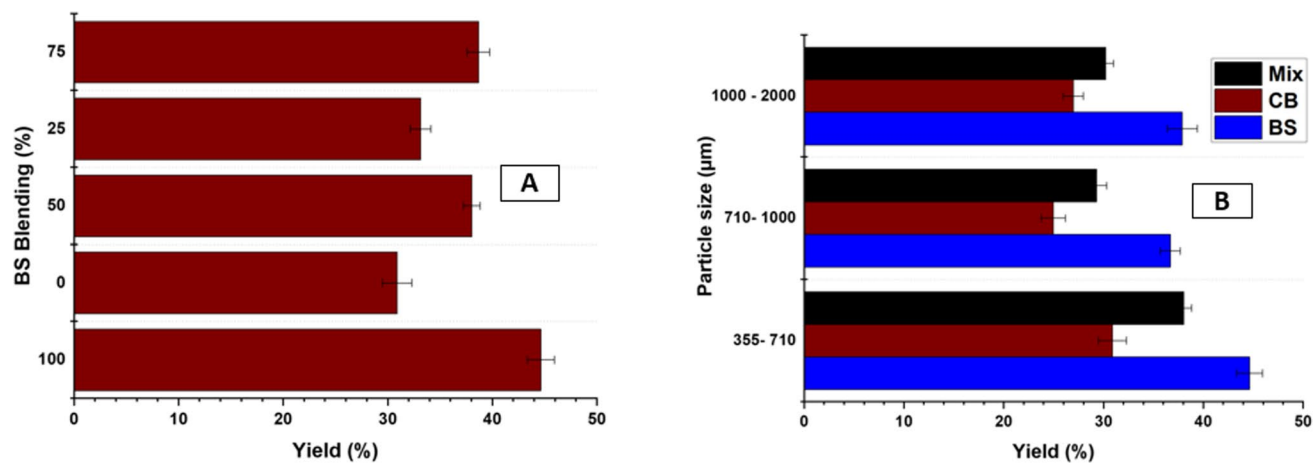


Fig. 4 Biochar yield effect by varying **A** particle size **B** blending ratio



RT on biochar yields is more gradual (Fig. 3C). Furthermore, statistically, the correlation test (at the 95% confidence level) reveals that a significant, strong negative correlation was only observed with varying temperatures (-0.877 , -0.776 , -0.844 for BS, CB, and mixed samples, respectively) (Table S3). This study's results are similar to another parametric study on rapeseed biochar, which concluded temperature as the only parameter that showed statistical significance on biochar yield (Zhao et al. 2018). Generally, mixing lignocellulosic and other biomasses with SS are known to reduce the yield of the samples. A study on mixing feedstocks such as bamboo wastes, rice husk, kitchen waste, wood sawdust, and exhausted tea wastes with SS reported reduced yield in all cases (Wang et al. 2021)—this is true for all conditions in the present study as well (Fig. 3).

The effect of varying particle size was also conducted to understand if there is a significant impact, as mentioned in “Feedstock characterization” section. From observations, it is clear that there is a slightly better yield when the smallest particle size samples (355–710 μm) were pyrolyzed—this is consistent with all samples (Fig. 4B). A similar study on bamboo chars concluded that the heat transfer and diffusion paths in smaller particle size samples aid in increased char production (Parthasarathy et al. 2021; Mariyam et al. 2023). However, this difference was not proven to be statistically significant.

On the contrary, the effect of the blending ratio was statistically proven significant, and a strong negative correlation with yield (at a 95% confidence interval) was demonstrated (Table S3)—this indicates that when the amount of BS decreased (increased CB), the yield reduced significantly. This is expected as the yield of

BS at all conditions studied was much higher than CB. Figure 4A shows that the yield is in the following order $\text{Mix}_{25} < \text{Mix}_{50} < \text{Mix}_{75}$. This could occur because CB has a higher volatile content than BS (Table S1), producing a higher oil and gas yield than char. This is consistent with literature that explains a lower ash and high volatile content in lignocellulosic biomass tends to produce more oil and gas and a lower char content (Imam and Capareda 2012).

Effect of pyrolysis temperature on ash content, metal concentration, and surface charge

The ash content in the biochar increased with rise in pyrolysis temperature (Fig. 5). The possible decomposition of the volatile organic matter and the presence of non-volatile mineral components led to increased ash production (Aktar et al. 2022). At lower temperatures, BS char has a comparatively higher amount of ash, but CB was observed to have higher ash as the temperature increased and this could be due to a higher loss of volatiles in CB at higher temperatures as both feedstock type and temperature are known to play a key role in the ash content produced (Crombie et al. 2013) (Fig. 5). In all cases, the ash content in the mixed samples remained between the BS and CB samples range. In a similar fashion, the zeta potential values reveals that the surface charge of the samples increases as the pyrolysis temperature increases (Fig. 5). The char samples' negativity shows the potential for attracting positively charged pollutants from water or other sources. A similar trend of increased positivity with temperature is described in the literature (Julien et al. 1998; Suliman et al. 2016).

The effect of temperature on metal concentration was studied at 450, 550, and 650 $^{\circ}\text{C}$, and the results revealed that the metal became more concentrated as the temperature increased (Table S4). Previous work has also reported the accumulation of metals with an increase in pyrolysis temperature due to the reduced weight loss of metals compared to organic compounds at higher temperatures (Lu et al. 2016; Wang et al. 2019b). Like the feeds, selenium, arsenic, and cadmium were not detected in any of the samples (in section “Yield calculations”), and iron and zinc were observed to have the highest concentration. Zinc and other metals like copper and lead are considered high contributors in the sludge char samples based on the source (Xingdong Wang et al. 2019a, b; Tytla 2019). Even though zinc is regarded as an essential pollutant, its environmental risk is considered insignificant at times (Tytla 2019), showing unproblematic metal mobility due to the alkaline nature of SS samples (Wang et al. 2019a). Therefore, further toxicity tests must be

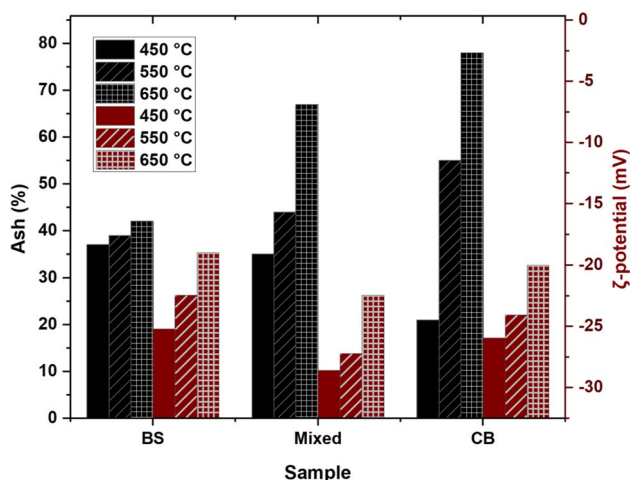


Fig. 5 Pyrolysis temperature effect on ash content and surface charge



Table 3 Pyrolysis temperature effect on mean elemental concentration in %

Sample	Pyrolysis temperature	C	H	N	S
BS	350	33.62	2.90	5.20	5.81
	450	43.87	2.90	5.35	5.45
	550	35.85	2.61	5.33	5.62
	650	43.55	1.37	6.12	5.12
	750	43.87	1.13	6.36	6.43
CB	850	44.02	1.01	6.56	6.43
	350	44.94	1.61	0.08	3.12
	450	48.96	1.58	0.05	3.96
	550	49.40	1.54	0.10	3.81
	650	49.54	1.37	0.08	3.23
Mix	750	49.67	1.38	0.08	3.20
	850	50.00	1.24	0.03	3.41
	350	38.97	1.80	5.05	4.51
	450	39.34	1.63	5.65	4.21
	550	40.34	1.54	5.32	3.67
	650	46.39	1.34	5.21	3.89
	750	47.39	1.21	5.01	4.02
	850	49.39	1.03	5.42	4.31

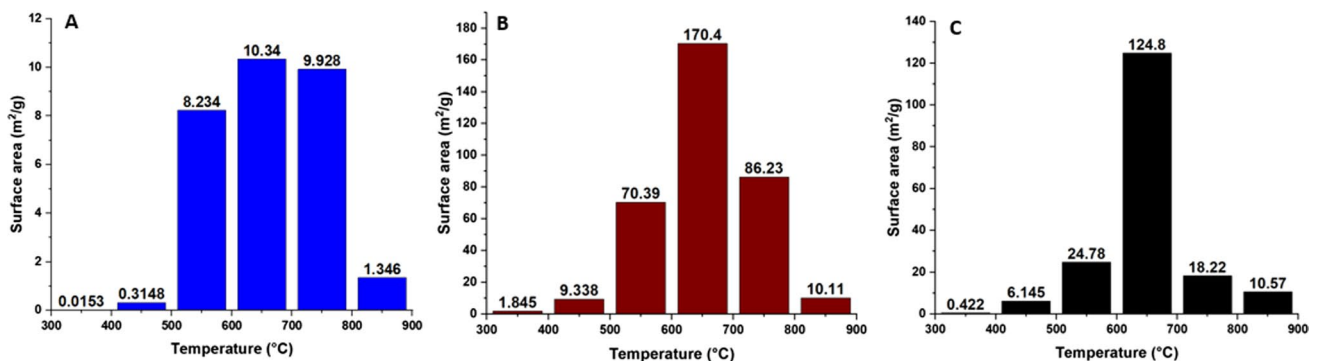
considered before water treatment, or other applications affecting the environment. As anticipated, CB samples are less polluted by metals. However, mixed samples are again seen to contain high amounts of iron due to the influence of BS (Table S4).

Effect of factors on elemental composition

Compared to the feeds, the carbon content is significantly higher in the char samples, especially those produced at high temperatures (Table 3). The elemental composition of the samples changes with the increase in temperature for all three samples. As temperature increases, the carbon content also does with the maximum carbon content in CB at 50%. Additionally, mixed samples had carbon ranges between BS and CB at each stage. Alternatively, the presence of hydrogen decreased with an increase in temperature. Sulfur was detected in all the char samples, unlike the feedstocks, which is compliant with some reported research showing less sulfate and more sulfur at higher pyrolytic temperatures (500–800 °C)—the reason is attributed to the changes in composition and speciation of the

Table 4 Comparison of surface area of biochar samples with literature

Feedstock	Operating conditions	Surface area (m ² /g)	Reference
SS	Temp: 550 °C	0.920	(Wang et al. 2021)
SSB	HR: 10 °C/min	31.3	
SSB with bamboo sawdust	RT: 60 min	20.3	
SSB with wood sawdust		14.7	
SSB with exhausted tea		22.1	
SSB with rice husk		16.0	
SSB with kitchen waste		12.1	
BS	Temp: 550 °C	8.234	This study
CB	HR: 5 °C/min	70.39	
Mixed	RT: 120 min	24.78	

**Fig. 6** Effect of temperature on mean surface area of samples A BS B CB C Mixed

biochar when the pyrolysis temperature increases (Cheah et al. 2014). The effect of HR and RT is not evident, as only minimal changes are observed with varying parameters (Table S5). A similar study on the “effect of pyrolysis temperature, heating rate, and residence time on rapeseed stem” also concluded temperature to be the only significant factor contributing to the char samples' elemental composition. Likewise, only a minimal effect is observed with varying particle size of the feeds (Table S5). Furthermore, Table S5 shows the impact of the blending ratio on the elemental composition—the higher the CB in the mix, the greater the carbon content following the order: $Mix_{75} < Mix_{50} < Mix_{25}$.

Effect of factors on surface area of biochar

The results obtained from this study are in accordance with the literature in that the SA of the biochar at 550 °C is much higher compared to the feedstock (Table S6). Contrary to the reported paper in Table 4, this study reveals that the SA improved significantly when mixed with CB. Furthermore, the SA for all three samples increased with temperature rise (Fig. 6). This observation has been reported in the literature several times and described in a review paper (Paz-Ferreiro et al. 2018). Temperature is known to cause changes in biochar SA and porosity mainly caused by the organic matter decomposition forming micropores; additionally, the aliphatic alkyls and ester groups destroy, under high temperatures, exposing the aromatic lignin, which is known to increase the SA (Wang et al. 2020). However, temperatures above 550 °C showed a reduction in the SA, possibly due to the high ash content as described in a paper comparing biomass char and ash (Trivedi et al. 2018) (Fig. 6). This result is also supported by a recent article with similar results (Xu et al. 2017), explaining the possible collapsing of micropores caused by the loss of volatiles with additional reduction in SA due to the sintering process at higher temperatures (Lu et al. 1995).

Furthermore, HR and RT have shown minimal effects on SA, concluding temperature to be the main effecting parameter (Table S6). The particle size study at 450 °C showed minimal effects on the SA. However, varying blending ratio revealed that the SA increased from 1.425 m²/g to 8.338 m²/g when 25% and 75% of CB were mixed with BS, respectively. Regarding the blending ratio study, the maximum SA of 9.338 m²/g was obtained when CB was pyrolyzed without mixing with BS.

Conclusion

This study uniquely focused on pyrolyzing biosolid, cardboard, and mixed samples to understand the properties of the biochar obtained. TGA showed that the degradation behavior of all three samples is similar, showing significant weight loss between 400 and 500 °C; this is evident in the calculated yield as a factor of temperature. The biochar yield was in the order $BS > Mix > CB$ for all conditions. Statistically, only temperature and blending ratio were shown to have a significant yield effect showing reduced yields when the temperature and cardboard content increased. However, by observation, a negative yield effect was shown when heating rate, residence time and particle size increased. In terms of surface area, the maximum was found to be 650 °C, revealing 10.34, 170.4 and 124.8 m²/g for BS, CB and mixed samples, respectively. Nevertheless, the ash content for these samples is high and the yield is low. Just like the biochar yield, temperature and blending ratio are shown to be the conditions to have a more pronounced effect on the surface area and elemental composition. Finally, a rise in temperature is shown to increase the surface charge and metal concentration. Considering all the yield studies and characterization of the biochar samples, the ones produced at 450 °C can be regarded as most suitable for further upgrading and environmental applications. Since the heating rate and residence time did not show pronounced effects, a heating rate 5 °C/min and residence time of 30 min can be considered for future applications. The proximate and ultimate analyses of the biochar samples produced at these conditions are shown in Table S7. The produced biochar can be activated to improve functionality and surface properties to enable water treatment applications or be used directly for agricultural purposes. For proper application of the biochar samples, leaching studies needs to be conducted to check if the environmental regulation limits are met. The presence of iron in the BS and mixed samples can also be used to advantage for pollutant removal studies owing to the iron content and magnetic properties.

Supplementary Information The online version contains supplementary material available at <https://doi.org/10.1007/s13762-023-04963-0>.

Acknowledgements The authors would like to acknowledge the financial support provided by Qatar National Research Fund and Hamad Bin Khalifa University. A special appreciation is expressed to Qatar Shell Research and Technology Center—Qatar for the collaboration and providing with the BS samples and Mr. Ojima Zechariah Wada from Hamad Bin Khalifa University for supporting the statistical analysis in this study. Any opinions, findings and conclusions, or recommendations expressed in this material are those of the authors and do not necessarily reflect the views of any of the parties. Finally, the authors



would also like to express thanks to Qatar National Library for access to articles.

Author's contributions The first author, SZ contributed to the conceptualization, methodology, and formal analysis and writing the original draft. The methodology, investigation, and visualization were further conducted by Dr. SP and finally Prof. GM reviewed and edited the manuscript in addition to supervising the study.

Funding Open Access funding provided by the Qatar National Library. This work was supported by funding from Qatar National Research Fund NPRP11S-0117-180328 and Hamad Bin Khalifa University.

Data availability Research data if not available in the supplementary material can be obtained from the corresponding author through email.

Declarations

Conflict of interest The authors have no competing interests to declare that are relevant to the content of this article.

Ethical approval This article does not contain any studies with human participants performed by any of the authors.

Open Access This article is licensed under a Creative Commons Attribution 4.0 International License, which permits use, sharing, adaptation, distribution and reproduction in any medium or format, as long as you give appropriate credit to the original author(s) and the source, provide a link to the Creative Commons licence, and indicate if changes were made. The images or other third party material in this article are included in the article's Creative Commons licence, unless indicated otherwise in a credit line to the material. If material is not included in the article's Creative Commons licence and your intended use is not permitted by statutory regulation or exceeds the permitted use, you will need to obtain permission directly from the copyright holder. To view a copy of this licence, visit <http://creativecommons.org/licenses/by/4.0/>.

References

- Aktar S, Hossain MA, Rathnayake N et al (2022) Effects of temperature and carrier gas on physico-chemical properties of biochar derived from biosolids. *J Anal Appl Pyrolysis* 164:105542. <https://doi.org/10.1016/j.jaap.2022.105542>
- Ayyadurai S, Arunachalam KD (2022) Experimental investigations on sugarcane bagasse pyrolytic oil production from flash pyrolysis using a rotary screw reactor. *Biofuels Bioprod Biorefining* 16:576–586. <https://doi.org/10.1002/bbb.2330>
- Bai J, Fu X, Lv Q et al (2021) Co-pyrolysis of sewage sludge and pinewood sawdust: the synergistic effect and bio-oil characteristics. *Biomass Convers Biorefinery*. <https://doi.org/10.1007/s13399-021-01809-y>
- Brindhadevi K, Anto S, Rene ER et al (2021) Effect of reaction temperature on the conversion of algal biomass to bio-oil and biochar through pyrolysis and hydrothermal liquefaction. *Fuel* 285:119106. <https://doi.org/10.1016/j.fuel.2020.119106>
- Callegari A, Capodaglio AG (2018) Properties and beneficial uses of (bio)chars, with special attention to products from sewage sludge pyrolysis. *Resources* 7:20. <https://doi.org/10.3390/resour7010020>
- Cheah S, Malone SC, Feik CJ (2014) Speciation of sulfur in biochar produced from pyrolysis and gasification of oak and corn stover. *Environ Sci Technol* 48:8474–8480. <https://doi.org/10.1021/es500073r>
- Chow HY, Pan M (2020) Fertilization value of biosolids on nutrient accumulation and environmental risks to agricultural plants. *Water Air Soil Pollut* 231:578. <https://doi.org/10.1007/s11270-020-04946-8>
- Collivignarelli MC, Canato M, Abbà A, Carnevale Miino M (2019) Biosolids: what are the different types of reuse? *J Clean Prod* 238:117844. <https://doi.org/10.1016/j.jclepro.2019.117844>
- Crombie K, Sohi SP, Brownsort P, Cross A (2013) The effect of pyrolysis conditions on biochar stability as determined by three methods. *Gcb Bioenergy* 5:122–131. <https://doi.org/10.1111/gcbb.12030>
- Fakayode OA, Aboagrib EAA, Zhou C, Ma H (2020) Co-pyrolysis of lignocellulosic and macroalgae biomasses for the production of biochar—a review. *Bioresour Technol* 297:122408. <https://doi.org/10.1016/j.biortech.2019.122408>
- Gopinath A, Divyapriya G, Srivastava V et al (2021) Conversion of sewage sludge into biochar: a potential resource in water and wastewater treatment. *Environ Res* 194:110656. <https://doi.org/10.1016/j.envres.2020.110656>
- Imam T, Capareda S (2012) Characterization of bio-oil, syn-gas and bio-char from switchgrass pyrolysis at various temperatures. *J Anal Appl Pyrolysis* 93:170–177. <https://doi.org/10.1016/j.jaap.2011.11.010>
- Julien F, Baudu M, Mazet M (1998) Relationship between chemical and physical surface properties of activated carbon. *Water Res* 32:3414–3424. [https://doi.org/10.1016/S0043-1354\(98\)00109-2](https://doi.org/10.1016/S0043-1354(98)00109-2)
- Kazemi Targhi N, Tavakoli O, Nazemi AH (2022) Co-pyrolysis of lentil husk wastes and *Chlorella vulgaris*: bio-oil and biochar yields optimization. *J Anal Appl Pyrolysis* 165:105548. <https://doi.org/10.1016/j.jaap.2022.105548>
- Kogbara RB, Yiming W, Iyengar SR et al (2020) Recycling industrial biosludge for buffel grass production in Qatar: impact on soil, leachate and plant characteristics. *Chemosphere* 247:125886. <https://doi.org/10.1016/j.chemosphere.2020.125886>
- Li J, Yu G, Pan L et al (2020) Ciprofloxacin adsorption by biochar derived from co-pyrolysis of sewage sludge and bamboo waste. *Environ Sci Pollut Res* 27:22806–22817. <https://doi.org/10.1007/s11356-020-08333-y>
- Liu J, Hou Q, Ju M et al (2020) Biomass pyrolysis technology by catalytic fast pyrolysis, catalytic co-pyrolysis and microwave-assisted pyrolysis: a review. *Catalysts* 10:1–26. <https://doi.org/10.3390/catal10070742>
- Lu GQ, Low JCF, Liu CY, Lua AC (1995) Surface area development of sewage sludge during pyrolysis. *Fuel* 74:344–348. [https://doi.org/10.1016/0016-2361\(95\)93465-P](https://doi.org/10.1016/0016-2361(95)93465-P)
- Lu T, Yuan H, Wang Y et al (2016) Characteristic of heavy metals in biochar derived from sewage sludge. *J Mater Cycles Waste Manag* 18:725–733. <https://doi.org/10.1007/s10163-015-0366-y>
- Mariyam S, Shahbaz M, Al-Ansari T et al (2022) A critical review on co-gasification and co-pyrolysis for gas production. *Renew Sustain Energy Rev* 161:112349. <https://doi.org/10.1016/j.rser.2022.112349>
- Mariyam S, Al-Ansari T, McKay G (2023) Particle size impact on pyrolysis of multi-biomass: a solid-state reaction modeling study. *Energy Sour Part A Recover Util Environ Eff*. <https://doi.org/10.1080/15567036.2023.2196945>
- Mašek O, Brownsort P, Cross A, Sohi S (2013) Influence of production conditions on the yield and environmental stability of



- biochar. *Fuel* 103:151–155. <https://doi.org/10.1016/j.fuel.2011.08.044>
- Mohamed BA, Li LY (2022) Biofuel production by co-pyrolysis of sewage sludge and other materials: a review. *Environ Chem Lett* 21:153–182. <https://doi.org/10.1007/s10311-022-01496-9>
- Morf L, Schlumberger S, Adam F, Díaz Nogueira G (2018) Urban phosphorus mining in the canton of Zurich: Phosphoric acid from sewage sludge ash. *Phosphorus Recovery Recycl*. https://doi.org/10.1007/978-981-10-8031-9_10
- Nowicki P, Kazmierczak-Razna J, Skibiszewska P et al (2016) Production of activated carbons from biodegradable waste materials as an alternative way of their utilisation. *Adsorption* 22:489–502. <https://doi.org/10.1007/s10450-015-9719-z>
- Parthasarathy P, Mackey HR, Mariyam S et al (2021) Char products from bamboo waste pyrolysis and acid activation. *Front Mater* 7:624791. <https://doi.org/10.3389/fmats.2020.624791>
- Patel S, Kundu S, Halder P et al (2019) Thermogravimetric Analysis of biosolids pyrolysis in the presence of mineral oxides. *Renew Energy* 141:707–716. <https://doi.org/10.1016/j.renene.2019.04.047>
- Paz-Ferreiro J, Nieto A, Méndez A et al (2018) Biochar from biosolids pyrolysis: a review. *Int J Environ Res Public Health* 15:956. <https://doi.org/10.3390/ijerph15050956>
- Racek J, Sevcik J, Chorazy T et al (2020) Biochar—recovery material from pyrolysis of sewage sludge: a review. *Waste Biomass Valoriz* 11:3677–3709
- Raju NJ (2016) Geostatistical and geospatial approaches for the characterization of natural resources in the environment. Springer, Berlin, p 969. <https://doi.org/10.1007/978-3-319-18663-4>
- Rathnayake D, Ehidihamhen PO, Eugene CE et al (2021) Investigation of biomass and agricultural plastic co-pyrolysis: effect on biochar yield and properties. *J Anal Appl Pyrolysis* 155:105029. <https://doi.org/10.1016/j.jaap.2021.105029>
- Rio S, Le Coq L, Faur C et al (2006) Preparation of adsorbents from sewage sludge by steam activation for industrial emission treatment. *Process Saf Environ Prot* 84:258–264. <https://doi.org/10.1205/psep.05161>
- Sakulkit P, Palamanit A, Dejchanchaiwong R, Reubroycharoen P (2020) Characteristics of pyrolysis products from pyrolysis and co-pyrolysis of rubber wood and oil palm trunk biomass for bio-fuel and value-added applications. *J Environ Chem Eng* 8:104561. <https://doi.org/10.1016/j.jece.2020.104561>
- Salvador S, Quintard M, David C (2004) Combustion of a substitution fuel made of cardboard and polyethylene: influence of the mix characteristics—experimental approach. *Fuel* 83:451–462. <https://doi.org/10.1016/j.fuel.2003.10.004>
- Saravanakumar A, Chen WH, Arunachalam KD et al (2022) Pilot-scale study on downdraft gasification of municipal solid waste with mass and energy balance analysis. *Fuel* 315:123287. <https://doi.org/10.1016/j.fuel.2022.123287>
- Sotoudehnia F, Baba Rabiou A, Alayat A, McDonald AG (2020) Characterization of bio-oil and biochar from pyrolysis of waste corrugated cardboard. *J Anal Appl Pyrolysis* 145:104722. <https://doi.org/10.1016/j.jaap.2019.104722>
- Sotoudehnia F, Mengistie E, Alayat A, McDonald AG (2021) Valorization of waste waxed corrugated cardboard via pyrolysis for recovering wax. *Environ Prog Sustain Energy* 40:1–13. <https://doi.org/10.1002/ep.13566>
- Sukarta IN, Sastrawidana IDK, Ayuni NPS (2018) Proximate analysis and calorific value of pellets in biosolid combined with wood waste biomass. *J Ecol Eng* 19:185–190. <https://doi.org/10.12911/22998993/86153>
- Suliman W, Harsh JB, Abu-Lail NI et al (2016) Influence of feedstock source and pyrolysis temperature on biochar bulk and surface properties. *Biomass Bioenerg* 84:37–48. <https://doi.org/10.1016/j.biombioe.2015.11.010>
- Suo F, You X, Yin S et al (2021) Preparation and characterization of biochar derived from co-pyrolysis of *Enteromorpha prolifera* and corn straw and its potential as a soil amendment. *Sci Total Environ* 798:149167. <https://doi.org/10.1016/j.scitotenv.2021.149167>
- Suthar S, Kishore Singh N (2022) Fungal pretreatment facilitates the rapid and valuable composting of waste cardboard. *Bioresour Technol* 344:126178. <https://doi.org/10.1016/j.biortech.2021.126178>
- Thibanyane N, Agachi P, Danha G (2019) Effects of biomass/coal copyrolysis parameters on the product yield: a review. *Procedia Manuf* 35:477–487. <https://doi.org/10.1016/j.promfg.2019.07.007>
- Trivedi NS, Mandavgane SA, Chaurasia A (2018) Characterization and valorization of biomass char: a comparison with biomass ash. *Environ Sci Pollut Res* 25:3458–3467. <https://doi.org/10.1007/s11356-017-0689-4>
- Tytla M (2019) Assessment of heavy metal pollution and potential ecological risk in sewage sludge from municipal wastewater treatment plant located in the most industrialized region in Poland—case study. *Int J Environ Res Public Health* 16:1–16. <https://doi.org/10.3390/ijerph16132430>
- Wang X, Deng S, Tan H et al (2016) Synergetic effect of sewage sludge and biomass co-pyrolysis: a combined study in thermogravimetric analyzer and a fixed bed reactor. *Energy Convers Manag* 118:399–405. <https://doi.org/10.1016/j.enconman.2016.04.014>
- Wang X, Chi Q, Liu X, Wang Y (2019a) Influence of pyrolysis temperature on characteristics and environmental risk of heavy metals in pyrolyzed biochar made from hydrothermally treated sewage sludge. *Chemosphere* 216:698–706. <https://doi.org/10.1016/j.chemosphere.2018.10.189>
- Wang X, Li C, Li Z et al (2019b) Effect of pyrolysis temperature on characteristics, chemical speciation and risk evaluation of heavy metals in biochar derived from textile dyeing sludge. *Ecotoxicol Environ Saf* 168:45–52. <https://doi.org/10.1016/j.ecoenv.2018.10.022>
- Wang S, Zhang H, Huang H et al (2020) Influence of temperature and residence time on characteristics of biochars derived from agricultural residues: a comprehensive evaluation. *Process Saf Environ Prot* 139:218–229. <https://doi.org/10.1016/j.psep.2020.03.028>
- Wang X, Chang VWC, Li Z et al (2021) Co-pyrolysis of sewage sludge and organic fractions of municipal solid waste: Synergistic effects on biochar properties and the environmental risk of heavy metals. *J Hazard Mater* 412:125200. <https://doi.org/10.1016/j.jhazmat.2021.125200>
- Wantaneeyakul N, Kositkanawuth K, Turn SQ, Fu J (2021) Investigation of biochar production from copyrolysis of rice husk and plastic. *ACS Omega* 6:28890–28902. <https://doi.org/10.1021/acsomega.1c03874>
- Xu Q, Tang S, Wang J, Ko JH (2017) Pyrolysis kinetics of sewage sludge and its biochar characteristics. *Pyrolysis kinetics of sewage sludge and its biochar characteristics*. *Process Saf Environ Prot* 115:49–56. <https://doi.org/10.1016/j.psep.2017.10.014>
- Yogalakshmi KN, PD T, Sivashanmugam P et al (2022) Chemosphere lignocellulosic biomass-based pyrolysis : a comprehensive review. *Chemosphere* 286:131824. <https://doi.org/10.1016/j.chemosphere.2021.131824>



Zhang J, Jin J, Wang M et al (2020) Co-pyrolysis of sewage sludge and rice husk/ bamboo sawdust for biochar with high aromaticity and low metal mobility. *Environ Res* 191:110034. <https://doi.org/10.1016/j.envres.2020.110034>

Zhao B, O'Connor D, Zhang J et al (2018) Effect of pyrolysis temperature, heating rate, and residence time on rapeseed stem derived biochar. *J Clean Prod* 174:977–987. <https://doi.org/10.1016/j.jclepro.2017.11.013>

Authors and Affiliations

S. Zuhara¹  · S. Pradhan¹ · G. McKay¹

✉ S. Zuhara
szuhara@hbku.edu.qa

¹ Division of Sustainable Development, College of Science and Engineering, Hamad Bin Khalifa University, Education City, Qatar Foundation, Doha, Qatar

